Exploring the Limits of the Zintl Concept for the $A_{14}MPn_{11}$ Structure Type with M = Zn, Cd

Dianna M. Young,† Charles C. Torardi,‡ Marilyn M. Olmstead,† and Susan M. Kauzlarich*,†

Department of Chemistry, University of California, Davis, California 95616, and DuPont Central Research and Development, Experimental Station, Wilmington, Delaware 19880-0356

Received June 29, 1994. Revised Manuscript Received September 12, 1994®

$A_{14}ZnSb_{11+x}$ and $A_{14}CdSb_{11+x}$ (A = Ca, Sr) are synthesized by reacting elements in a 14:1:11 ratio at 1000 °C. Low-temperature (130 K) single-crystal X-ray diffraction data shows that these compounds are tetragonal, space group $I4_1/acd$, $Z = 8$, and are structurally similar to previously studied $A_{14}MPn_{11}$ (A = Ca, Sr, Ba; M = Al, Ga, Mn; Pn = As, Sb, Bi) compounds. However, these Zn and Cd compounds with the exception of $Sr_{14}ZnSb_{11}$ contain additional Sb and cannot be understood according to simple Zintl electron counting rules. Low-temperature lattice parameters, R1(wR2) are $Ca_{14}ZnSb_{11.20}$, a = 16.778 (3), c = 22.088 (6) Å, R1(wR2) = 0.063 (0.115); $Ca_{14}CdSb_{11.43}$, a = 16.583 (3), c = 23.167 (7) Å, R1(wR2) = 0.0353 (0.0792); $Sr_{14}ZnSb_{11}$, a = 17.569 (5), c = 22.961 (6) Å, R1(wR2) = 0.0486 (0.0997); $Sr_{14}CdSb_{11.37}$, a = 17.637 (3), c = 23.163 (4) Å, R1(wR2) = 0.0627 (0.1435). Temperature-dependent resistivity measurements show that these materials are semiconducting in behavior with small activation energies: $Ca_{14}ZnSb_{11.20}$: $E_a = 3.9(1) \times 10^{-3}$ eV; $Ca_{14}CdSb_{11.43}$, $E_a = 7.6(1) \times 10^{-2}$ eV; $Sr_{14}ZnSb_{11}$, $E_a = 1.5(1) \times 10^{-2}$ eV; $Sr_{14}CdSb_{11.37}$, $E_a = 1.1(1) \times 10^{-2}$ eV. Several simple models are presented in order to understand the crystallographic results.

Introduction

Establishing a basic understanding of structure–property relationships in compounds is an important aspect of solid-state chemistry. Zintl compounds are a class of compounds whose structure and bonding can be understood using valence rules.[1–4] A unique group of ternary Zintl compounds have the stoichiometry $A_{14}MPn_{11}$ (A = alkaline earth metals; M = group 13 or transition metals elements; Pn = group 15 elements), in which the first structure was determined for $Ca_{14}AlSb_{11}$.[5] To understand these ternary salt-like compounds, solid-state chemists use the Zintl or modified Zintl concept.[6] In brief, the Zintl concept is an electron counting scheme in which electropositive elements donate electrons to electronegative elements. These electronegative elements in turn use the transferred electrons to form bonds such that all elements satisfy the $(8 - N)$ rule.[7] Zintl phases are therefore considered to be composed of cations and covalently bonded polyatomic anions. They are usually semiconducting, although some Zintl phases have also been found to be metallic.[6]

To date, a number of $A_{14}MPn_{11}$ analogs have been studied. The main-group compounds, $A_{14}AlSb_{11}$ (A = Ca, Sr, Ba)[5,8] and $A_{14}GaAs_{11}$ (A = Ca, Sr),[9,10] have been investigated. $A_{14}GaAs_{11}$ and $Ca_{14}AlSb_{11}$ abide Zintl counting rules and are isostructural. $Sr_{14}AlSb_{11}$ and $Ba_{14}AlSb_{11}$ have been shown to have excess Sb and are deficient in Al.[8] Apparently some Sb^{3+} replaces Al^{3+} in the structure. In the $Ca_{14}AlSb_{11}$ structure type, one formula unit consists of 14 Ca^{2+} cations, an $[AlSb_4]^{9-}$ tetrahedron, a $[Sb_3]^{7-}$ linear unit, and 4 isolated Sb^{3-} atoms. Note that Al is formally considered to be in the +3 oxidation state and the 31 electrons transferred from Ca and Al are donated to the more electronegative Sb. The electron-counting scheme successfully accounts for a number of semiconducting main group (M^{3+}) analogs.[8–10] Figure 1 shows a perspective view of the unit cell. The stacking of the $AlSb_4$ tetrahedra and Sb_3 linear units can be clearly seen in Figure 1a. The isolated Sb^{3-} anions are more clearly identified in the nonperspective view shown in Figure 1b.

The Zintl concept has been extended to the transition metal $A_{14}MnPn_{11}$ (A = Ca, Sr, Ba; Pn = As, Sb, Bi) compounds,[11–13] in which the Mn is in the +3 oxidation state and has been shown to be isostructural to the main group analogs. The +3 oxidation state of the Mn is confirmed by temperature-dependent magnetic susceptibility studies.[11–14]

† University of California, Davis.
‡ DuPont Central Research and Development.
® Abstract published in *Advance ACS Abstracts,* October 15, 1994.

(1) Schäfer, H.; Eisenmann, B.; Müller, W. *Angew. Chem., Int. Ed. Engl.* **1973,** *12,* 694.
(2) Schäfer, H.; Eisenmann, B. *Rev. Inorg. Chem.* **1981,** *3,* 29.
(3) Schäfer, H. *J. Solid State Chem.* **1985,** *57,* 97.
(4) Nesper, R. *Angew. Chem., Int. Ed. Engl.* **1991,** *30,* 789.
(5) Cordier, G.; Schäfer, H.; Stelter, M. *Z. Anorg. Allg. Chem.* **1984,** *519,* 183.
(6) Nesper, R. *Prog. Solid State Chem.* **1990,** *20,* 1.
(7) Kjekshus, A.; Rakke, T. *Structure and Bonding*; Springer-Verlag: New York, 1974; Vol. 19, p 46.
(8) Brock, S. L.; Weston, L. J.; Olmstead, M. M.; Kauzlarich, S. M. *J. Solid State Chem.* **1993,** *107,* 513.
(9) Kauzlarich, S. M.; Thomas, M. M.; Odink, D. A.; Olmstead, M. M. *J. Am. Chem. Soc.* **1991,** *113,* 7205.
(10) Kauzlarich, S. M.; Kuromoto, T. Y. *Croat. Chem. Acta* **1991,** *64,* 343.
(11) Kauzlarich, S. M.; Kuromoto, T. Y.; Olmstead, M. M. *J. Am. Chem. Soc.* **1989,** *111,* 8041.
(12) Kuromoto, T. Y.; Kauzlarich, S. M.; Webb, D. J. *Chem. Mater.* **1992,** *4,* 435.
(13) Rehr, A.; Kuromoto, T. Y.; Kauzlarich, S. M.; Del Castillo, J.; Webb, D. J. *Chem. Mater.* **1994,** *6,* 93.

0897-4756/95/2807-0093$09.00/0 © 1995 American Chemical Society

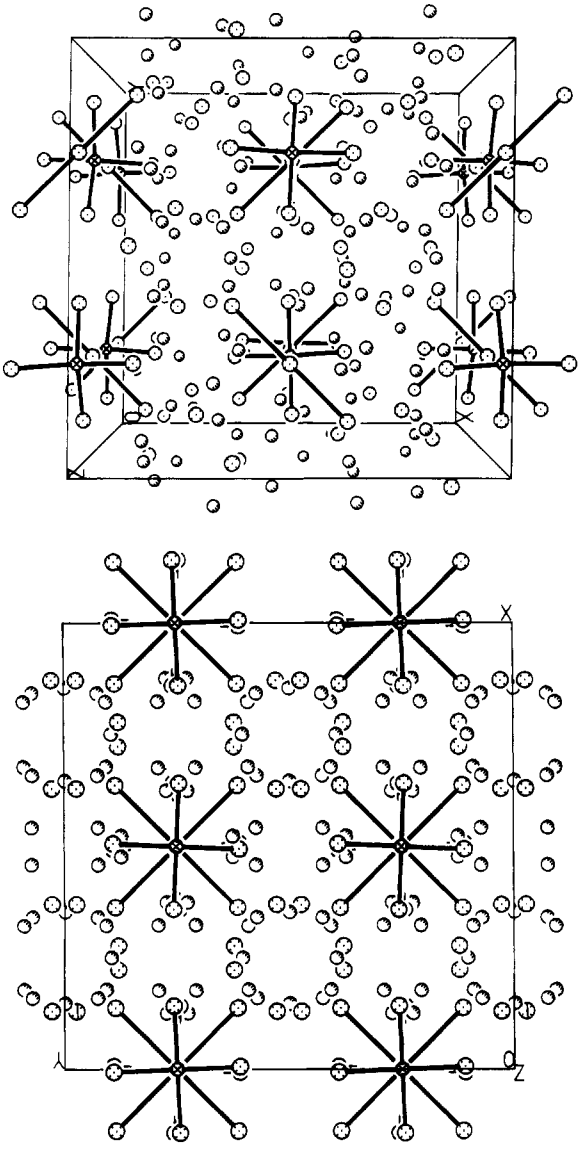

Figure 1. (a, top) Perspective view down the c axis. (b, bottom) [001] projection of the structure $Ca_{14}AlSb_{11}$, showing the relative orientation of the $AlSb_4$ tetrahedra, Sb_3 units, and Sb^{3-} anions in the cell. The Sb, Al, and Ca atoms are indicated by dotted, cross-hatched, and half-shaded circles, respectively.

We are interested in exploring the electronic constraints of this structure type, $A_{14}MPn_{11}$, where M can be any transition metal and have synthesized the compounds $A_{14}ZnSb_{11}$ and $A_{14}CdSb_{11}$ (A = Ca, Sr). Since Zn and Cd are expected to have a maximum formal oxidation state of +2, how will the electrons be counted according to the Zintl concept? This paper presents the synthesis, structures, and properties of these compounds and discusses various models for electron counting.

Experimental Section

Synthesis. All reactions were set up in an argon filled drybox. Ca, Sr, and Cd metals were cut into small pieces. $A_{14}MSb_{11}$ were prepared by adding stoichiometric amounts of the elements (Ca (99.99%, Anderson Physics Labs), Sr (99.9%, Strem Chemicals), Zn (99.4%, Fisher), Sb (99.999%, J. Matthey), Cd (99.9%, J. Matthey)) in a niobium tube which was sealed on one end. To investigate the possibility of an interstitial oxide, a few reactions were set up using ZnO (reagent grade, Aldrich) and CdO (reagent grade, Aldrich) in place of Zn and Cd. Several reactions were also set up with Sb_2O_3 (J. Matthey) as an additional reactant. The possibility of interstitial oxygen arose after various single-crystal X-ray refinements of $A_{14}MSb_{11+x}$ compounds and will be discussed in detail later. The niobium tube was first cleaned in an acid solution (20% HF, 25% HNO_3, and 55% H_2SO_4) and welded shut with an argon arc welder. After crimping the filled niobium tube shut, it was quickly transferred from the drybox to an argon arc welder to seal the other end. The niobium tube was then sealed in a quartz ampule under vacuum. The reactions were heated 60 °C/h to 1000 °C, maintained at that temperature for 300 h, and subsequently cooled at 20 °C/h to room temperature. The resulting air-sensitive products were typically made up of a mixture of highly reflective silver/black chunks of material, powder, and a small amount of long silver needle crystals. Guinier powder X-ray diffraction indicated that the majority (75−80%) of product was of the $Ca_{14}AlSb_{11}$ structure type. $A_{11}Sb_{10}$ was identified as an impurity.[15,16] Grinding the sample into a powder and reheating in niobium (as described above) at 1000 °C for 1−2 weeks provided quantitative yield (>95% based on Guinier powder X-ray diffraction) of $A_{14}MSb_{11}$ in the form of powder. The products were handled in a nitrogen filled drybox equipped with a microscope.

Elemental Analysis. Several single crystals were isolated in a nitrogen-filled drybox equipped with a microscope and pressed into indium. Under N_2 the sample was quickly transferred to a Cameca SX50 electron microprobe equipped with wavelength-dispersive spectrometers. The microprobe was operated with a 10 nA beam current and a 15 keV accelerating potential. The $Sr_{14}MSb_{11}$ compounds were too air sensitive to obtain well-defined smooth surfaces for microprobe analysis.

$Ca_{14}ZnSb_{11+x}$. Some decomposition of the crystal surfaces was apparent as determined from the lack of smooth surfaces on the crystal faces observed in the backscattered electron and reflected images. However, enough smooth surfaces were observed to conduct the analysis. Elemental analysis was based on 12 spots (1 μm in size) from two different crystals. There was no evidence of Nb in any of the crystals, which might have been present due to contamination from the Nb tubing used for the reaction containers. The presence of oxygen was of particular interest, but the counts for the oxygen peak were not significantly above the background. Ca, Zn, and Sb content were determined using $CaSiO_3$, pure Zn, and Freibergite ($Cu_7Fe_2Ag_3Sb_4S_{13}$) standards, respectively. The average total was 99.8(9)% weight for 12 spots. The result for the crystal are $Ca_{14.0(1)}Zn_{1.04(5)}Sb_{11.1(1)}$.

$Ca_{14}CdSb_{11+x}$. No decomposition of crystal surfaces was observed. One crystal was analyzed in which 15 spots (1 μm in size) were taken. There was no Nb detected and only trace amounts of O detected. The average total of the crystal was 99.8(6) wt %. Ca and Sb standards were the same as mentioned above. The standard used for Cd analysis was synthetic Cd sphalerite (0.1 CdS:0.9 ZnS). The results for the crystal is $Ca_{14.0(1)}Cd_{1.19(7)}Sb_{11.3(9)}$.

Powder X-ray Diffraction. Diffraction patterns were obtained with an Enraf-Nonius Guinier powder camera (monochromatic Cu $K\alpha_1$ radiation, wavelength 1.540 562 Å) at room temperature. Powder samples were prepared in a nitrogen-filled drybox in which the powder sample and NIST silicon standard were placed between two pieces of tape. Powder diffraction patterns were calculated with the program POWDER,[17] which uses atom positions obtained from single-crystal X-ray diffraction, and compared to the experimental powder diffraction patterns. Diffraction lines were measured with an

(14) Webb, D. J.; Kuromoto, T. Y.; Kauzlarich, S. M. *J. Magn. Magn. Mater.* **1991**, *98*, 71.

(15) Deller, K.; Eisenmann, B. *Z. Naturforsch.* **1976**, *31b*, 29.

(16) Rehr, A.; Kauzlarich, S. M. *Acta. Crystallogr.*, in press.

(17) Clark, C. M.; Smith, D. K.; Johnson, G. J., *POWDER*, FORTRAN II program for calculating X-ray diffraction patterns, Version 5, Department of Geosciences, Pennsylvania State University, University Park, PA, 1973.

Table 1. Crystallographic Parameters[a]

formula	$Ca_{14}ZnSb_{11.20}$	$Ca_{14}CdSb_{11.43}$	$Sr_{14}ZnSb_{11}$	$Sr_{11}CdSb_{11.37}$
fw	1990.95	2065.39	2631.32	2724.42
crystal size, mm	0.60 × 0.04 × 0.04	0.50 × 0.05 × 0.05	0.46 × 0.12 × 0.12	0.34 × 0.04 × 0.04
color and habitat	silver needle	silver needle	silver needle	silver needle
space group, Z	$I4_1/acd$	$I4_1/acd$	$I4_1/acd$	$I4_1/acd$
T, K	130	130	130	130
a, Å	16.778(3)	16.583(3)	17.569(5)	17.637(3)
c, Å	22.088(6)	23.167(7)	22.961(6)	23.163(7)
V, Å^3	6218(2)	6371(3)	7087(3)	7205(2)
μ (Mo Kα), mm^{-1}	12.447	12.374	29.741	29.179
ϱ_{calc}, Mg/m^3	4.200	4.292	4.932	4.938
rel trans factors, min/max	0.934−1.078	0.959−1.142	0.850−1.077	0.855−1.359
$2\theta_{max}$	55	55	55	55
octants collected	*hkl*	*hkl*	*hkl*	*hkl*
scan speed, deg/min	2.00	3.97	3.97	3.97
no. of data collected	3963	6401	4431	4587
no. of unique data	1795	1304	2035	2090
no. of obsd refns [$F_o > 4\sigma(F_o)$]	1315	1126	1537	1356
no. of params. refined	67	65	72	70
R1 [$I > 2\sigma(I)$][b]	6.30	3.53	4.86	6.27
wR2 [$I > 2\sigma(I)$][b]	11.15	7.92	9.97	14.35

[a] Room-temperature lattice parameters (obtained from Guinier powder diffraction): $Ca_{14}ZnSb_{11.20}$ a = 16.790(3), c = 22.022(6) Å; $Ca_{14}CdSb_{11.43}$ a = 16.595(4), c = 23.170(11) Å; $Sr_{14}ZnSb_{11}$ a = 17.632(2), c = 23.174(7) Å; $Sr_{14}CdSb_{11.37}$ a = 17.611(1), c = 23.277(3) Å.[b] R1 = $||F_o| - |F_c||/\Sigma|F_o|$ and wR2 = $\sqrt{(w(F_o^2 - F_c^2)^2/\Sigma wF_o^4)}$, $w = 1/[\sigma^2(F_o^2) + P^2 + P]$ where $P = (\max(F_o^2,0) + 2F_c^2)/3$.

Enraf-Nonius Guinier viewer and lines were converted to 2θ by standard nonlinear least-squares refinement using the program GUIN.[18] 2θ values were indexed using the program LATT[19] and room-temperature lattice parameters obtained. The lattice parameters for different reactions of each compound were, within standard deviations, the same. Room-temperature lattice parameters are given in Table 1. Tables of calculated versus experimental d spacings and intensities are provided as supplemental material.

Single-Crystal X-ray Diffraction. Suitable crystals were selected from each reaction in a nitrogen-filled drybox equipped with a microscope. The crystals were placed in Paratone oil to minimize air exposure. Each crystal selected for data collection was mounted on a glass fiber and quickly positioned on the diffractometer in which a cold stream of nitrogen protected it from air exposure. Data were collected on either a Siemens R3m or Syntex $P2_1$ diffractometer (Mo Kα, wavelength = 0.710 69 Å, graphite monochromator) at 130 K. The unit-cell dimensions and crystal system were determined by least-squares refinement of approximately 15−30 reflections ($10° < 2\theta < 35°$) using the automatic indexing routine of the diffractometer. Axial photos were taken at long exposure (30 min) to confirm Laue symmetry, cell dimensions, and to check for possible superstructure. Small data sets were taken (2θ = 25−35°) to confirm I centering. No decomposition of the crystals was observed during data collection based on the intensity of two check reflections monitored every 198 reflections. The space group determination was unambiguous. The data were corrected for Lorentz and polarization effects. The crystallographic parameters are summarized in Table 1. Crystallographic programs used were SHELXTL PLUS Version 4.21[20] and SHELXL-93.[21] In the SHELXL-93 program, F^2 is used in the refinement rather than F such that all data are used and typically the specified threshold for F is eliminated. The wR2 index is minimized during the refinement and is twice as large as the conventional R1 index due to all the data being used. Scattering factors and absorption coefficients used in SHELXL-93 are from the "International Tables for Crystallography".[22]

The $Sr_{14}ZnSb_{11}$ structure was solved and refined with the SHELXTL PLUS programs,[20] and the final refinements and absorption correction were performed in SHELXL-93.[21] The atoms were assigned to relevant intensity peaks and refined with isotropic U's. The structure of $Sr_{14}ZnSb_{11}$ was compared to $Ca_{14}AlSb_{11}$ and found to be similar. A residual peak of approximately 10 e$^-$/Å^3 remained in the Fourier difference map that was about 0.7 Å away from Sb(3). Since the peak was very close to Sb(3), it was attributed to positional disorder of Sb(3). This disorder is modeled as two atom sites Sb(3) and Sb(3′), which are partially occupied. The respective occupancies were restrained (total occupancy 1.0) and the refinement converged with occupancy for Sb(3) 0.85(1), and Sb(3′) 0.15(1). The thermal parameter for Sb(3) is slightly larger than that for Sb(3′) and was highly correlated. In addition, it was noted that the isotropic U for Sb(4) was approximately double the magnitude of the other Sb atoms. This large thermal parameter has been observed in a number of other compounds of the $Ca_{14}AlSb_{11}$ structure type.[8,10] A disorder model was employed similar to that used for $Sr_{14}GaAs_{11}$:[10] Sb(4), the central Sb atom in the linear chain, refined best in site 16f with a total occupancy 0.25 (half occupied). This model positions two Sb(4) atoms unreasonably close together (0.372(8) Å) but adequately accounts for the disorder in the Sb(4) position. No streaking or weak reflections which might be attributed to diffuse X-ray scattering or a superstructure were observed in the axial photos. An absorption correction[23] was applied after the isotropic refinement converged. In subsequent cycles, all atoms except Sb(3′) were refined with anisotropic U's. The final difference map was flat with the largest residual being ±2 e$^-$/Å^3. A second data set was collected on a $Sr_{14}ZnSb_{11}$ crystal from a different reaction. The refinement yielded similar results.

The remaining compounds, $Ca_{14}ZnSb_{11+x}$, $Sr_{14}CdSb_{11+x}$, and $Ca_{14}CdSb_{11+x}$, were refined with initial positions taken from $Sr_{14}ZnSb_{11}$, without the disordered position of Sb(3) or Sb(4). The refinements proceeded uneventfully, and an absorption correction was applied after convergence of the model with isotropic U's. A residual peak of about 10 e$^-$/Å^3 remained in the difference Fourier map. It was assigned as partial occupancy (5.2−10.8%) of an Sb atom (Sb(5)). Oxygen and other light atoms were also modeled in that site allowing no constraints on either the occupancy or the thermal parameters; although the R1, wR2 values were comparable for different models, the resulting isotropic U's were too small for the

(18) Imoto, H. *GUIN*, Fortran Program to calculate 2-theta from film with Si reference lines, Iowa State University, unpublished, 1979.
(19) Lii, K.; Wang, S.; Garcia, E. *LATT*, Iowa State University, unpublished, 1985.
(20) Sheldrick, G. M. *SHELXTL-PLUS, A Program for Crystal Structure Determination*, Version 4.21, Siemens Analytical X-ray Instruments, Madison, WI, 1990.
(21) Sheldrick, G. M. *SHELXL-93, J. Appl. Cryst.*, manuscript in preparation.
(22) Scattering factors (neutral atoms) are from *International Tables for X-ray Crystallography*; Reidel: Boston, 1992; Vol. C.
(23) Parkin, S.; Moezzi, B.; Hope, H. *XABS2*, program provides an empirical correction based on $F_o^2$and F_c^2 differences: *J. Appl. Cryst.*, in press.

Table 2. Structural Model Results for the Large Residual Peak Found in the $A_{14}MSb_{11}$ Structure

atom	K^a	U^b	R1[c]	wR2[c]
		$Ca_{14}ZnSb_{11.20}$		
O	0.350	0.002	0.063	0.120
Zn	0.074	0.014	0.062	0.117
Sb	0.051	0.026	0.063	0.115
		$Ca_{14}CdSb_{11.43}$		
O	0.749	0.000	0.036	0.102
Cd	0.114	0.017	0.035	0.083
Sb	0.107	0.018	0.035	0.079
		$Sr_{14}CdSb_{11.37}$		
O	0.646	0.000	0.063	0.165
Cd	0.100	0.012	0.062	0.164
Sb	0.094	0.013	0.062	0.143

[a] Site occupancy. [b] Refined isotropically. [c] $R1 = ||F_o| - |F_c||/\sum|F_o|$ and $wR2 = \sqrt{(w(F_o^2 - F_c^2)^2/\sum wF_o^4)}$, $w = 1/[\sigma^2(F_o^2) + P^2 + P]$ where $P = (\max(F_o^2,0) + 2F_c^2)/3$.

Table 3. Atomic Coordinates ($\times 10^4$) and Isotropic Equivalent Thermal Parameters ($Å^2 \times 10^3$)

atom	site	occupancy	x	y	z	U^b
			$Ca_{14}ZnSb_{11.20}$			
Sb(1)	16f	0.50	1362(1)	3862(1)	1250	13(1)
Sb(2)	32g	1.00	61(1)	1093(1)	8111(1)	14(1)
Sb(3)	32g	1.00	8711(1)	4726(1)	460(1)	19(1)
Sb(4)	8b	0.25	0	2500	1250	22(1)
Sb(5)[a]	32g	0.05	7565(14)	2742(13)	3316(10)	27(7)
Zn(1)	8a	0.25	0	2500	8750	14(1)
Ca(1)	32g	1.00	8241(2)	2915(2)	773(1)	17(1)
Ca(2)	32g	1.00	8755(2)	2266(2)	2469(2)	24(1)
Ca(3)	16e	0.50	8538(2)	0	2500	10(1)
Ca(4)	32g	1.00	8226(2)	4083(2)	3435(1)	21(1)
			$Ca_{14}CdSb_{11.43}$			
Sb(1)	16f	0.50	1356(1)	3856(1)	1250	13(1)
Sb(2)	32g	1.00	−23(1)	1097(1)	8016(1)	18(1)
Sb(3)	32g	1.00	8728(1)	9800(1)	9513(1)	21(1)
Sb(4)	8b	0.25	0	2500	1250	17(1)
Sb(5)[a]	16e	0.11	7500	8984(2)	10000	20(1)
Cd(1)	8a	0.25	0	2500	8750	17(1)
Ca(1)	32g	1.00	8224(1)	2948(1)	807(1)	26(1)
Ca(2)	32g	1.00	8773(1)	2280(1)	2406(1)	19(1)
Ca(3)	16e	0.50	8567(1)	0	2500	17(1)
Ca(4)	32g	1.00	8195(1)	3996(2)	3454(1)	46(1)
			$Sr_{14}ZnSb_{11}$			
Sb(1)	16f	0.50	1343(1)	3843(1)	1250	22(1)
Sb(2)	32g	1.0	46(1)	1125(1)	8129(1)	16(1)
Sb(3)	32g	0.85	8713(2)	9738(1)	9539(1)	21(1)
Sb(3′)	32g	0.15	8450(8)	9633(5)	9316(8)	13(3)
Sb(4)	16f	0.25	−75(3)	2425(3)	1250	17(2)
Zn(1)	8a	0.25	0	2500	8750	19(1)
Sr(1)	32g	1.00	8232(1)	2908(1)	774(1)	21(1)
Sr(2)	32g	1.00	8764(1)	2286(1)	2494(1)	24(1)
Sr(3)	16e	0.50	8547	0	2500	16(1)
Sr(4)	32g	1.00	8216(1)	4070(1)	3434(1)	24(1)
			$Sr_{14}CdSb_{11.37}$			
Sb(1)	16f	0.50	1347(1)	3847(1)	1250(10)	11(1)
Sb(2)	32g	1.00	61(1)	1081(1)	8111(1)	13(1)
Sb(3)	32g	1.00	8710(1)	9719(1)	9546(1)	17(1)
Sb(4)	16f	0.25	−93(3)	2407(3)	1250	21(2)
Sb(5)[a]	32g	0.09	5265(8)	−52(8)	−772(6)	13(4)
Cd(1)	8a	0.25	0	2500	8750	13(1)
Sr(1)	32g	1.00	8242(1)	2919(1)	777(1)	17(1)
Sr(2)	32g	1.00	8741(1)	2256(1)	2484(1)	25(1)
Sr(3)	16e	0.50	8531(1)	0	2500	10(1)
Sr(4)	32g	1.00	8230(1)	4076(1)	3441(1)	21(1)

[a] Refined isotropically. [b] Equivalent U_{iso} defined as one-third of the trace of the orthogonalized U_{ij} tensor.

assignment to be considered reasonable. Zn and Cd were also considered in that site, and the wR2 values in $Ca_{14}ZnSb_{11.20}$ and $Ca_{14}CdSb_{11.43}$ were nearly identical to Sb. However, in the case of $Sr_{14}CdSb_{11.37}$, the wR2 value increased considerably suggesting that Cd does not model the residual peak as well as Sb. In all three compounds Sb was determined to be the best choice for the residual peak based on coordination number and bond distances of neighboring cations and anions. The attempted models and results for all the compounds that exhibited a large residual peak are summarized in Table 2. In all cases, Sb(5) is surrounded by four cations at distances of 2.5−3.4 Å and three Sb atoms at distances of 2.6−3.2 Å. In the case of $Sr_{14}CdSb_{11.37}$, the isotropic U for Sb(4) was approximately double the magnitude of the other Sb atoms and Sb(4) was modeled similarly to that described above for $Sr_{14}ZnSb_{11}$. All atoms were refined with anisotropic U's except Sb(5) until convergence. Final difference maps were flat for all three compounds, in which $Sr_{14}CdSb_{11.43}$ exhibited the largest residual peak of ±4.0 $e^-/Å^3$. In $Ca_{14}ZnSb_{11.20}$ and $Ca_{14}CdSb_{11.37}$, the largest residual peaks were ±1.5 and ±3.8 $e^-/Å^3$, respectively. Tables of anisotropic U's, F_o's and F_c's are provided as supplementary material (see paragraph at end of paper). Positional parameters and isotropic U's are given in Table 3. Selected bond distances and angles are listed in Tables 4 and 5.

Table 4. Selected Bond Lengths (Å) and Angles (deg) for $Ca_{14}ZnSb_{11.20}$ and $Ca_{14}CdSb_{11.43}$

	$Ca_{14}ZnSb_{11.20}$	$Ca_{14}CdSb_{11.43}$
Sb(1)−Sb(4)	3.231(1)	3.180(1)
Sb(1)−Ca(1) × 2	3.232(3)	3.238(2)
Sb(1)−Ca(2) × 2	3.296(3)	3.281(2)
Sb(1)−Ca(3) × 2	3.361(1)	3.464(1)
Sb(1)−Ca(4) × 2	3.226(3)	3.135(2)
Sb(2)−M(1)	2.752(1)	2.882(1)
Sb(2)−Ca(1)	3.199(3)	3.174(2)
Sb(2)−Ca(1′)	3.215(3)	3.204(2)
Sb(2)−Ca(2)	3.136(3)	3.184(2)
Sb(2)−Ca(2′)	3.794(4)	3.636(2)
Sb(2)−Ca(3)	3.273(3)	3.251(2)
Sb(2)−Ca(4)	3.175(3)	3.128(2)
Sb(2)−Ca(4′)	3.368(3)	3.513(3)
Sb(3)−Ca(1)	3.214(3)	3.229(2)
Sb(3)−Ca(1′)	3.254(3)	3.268(2)
Sb(3)−Ca(2)	3.182(3)	3.180(2)
Sb(3)−Ca(2′)	3.301(4)	3.289(2)
Sb(3)−Ca(3)	3.163(3)	3.137(2)
Sb(3)−Ca(4)	3.259(3)	3.285(2)
Sb(3)−Ca(4′)	3.798(4)	3.458(3)
Sb(4)−Ca(1) × 4	3.211(3)	3.206(2)
Sb(4)−Ca(2) × 4	3.430(3)	3.383(2)
Sb(5)−Sb(1)	2.920(22)	
Sb(5)−Sb(2)	2.948(22)	3.258(3) × 2
Sb(5)−Sb(3)	2.746(21)	2.693(2) × 2
Sb(5)−Sb(3)	3.339(21)	
Sb(5)−Ca(1)	2.664(22)	2.810(3) × 2
Sb(5)−Ca(2)	2.850(22)	
Sb(5)−Ca(2′)	2.812(23)	
Sb(5)−Ca(3)		3.453(5)
Sb(5)−Ca(4)		2.817(3) × 2
Sb(2)−M−Sb(2′)	105.26(2)	107.63(3)
Sb(2)−M−Sb(2″)	118.96(4)	110.40(1)

Second data sets were collected for crystals of $Ca_{14}ZnSb_{11+x}$, $Ca_{14}CdSb_{11+x}$, and $Sr_{14}CdSb_{11+x}$ obtained from different reactions. A half-sphere of data ($2\theta_{max} = 55°$) was collected for $Ca_{14}ZnSb_{11+x}$. An empirical absorption correction, XEMP,[24] was used with this data set in order to ascertain whether the residual peak was simply due to inadequate absorption correction. The refinement proceeded uneventfully with isotropic U's for all atoms as described above. The large residual peak in the Fourier difference map of approximately 10 $e^-/Å^3$ was again present in the same position as observed for the first data set. As before, after exploring the effect of light atoms and the metals Zn and Cd, the 10 $e^-/Å^3$ peak was best modeled as a nonstoichiometric amount of Sb (5.2% occupancy) for the same reasons as given above.

In addition, a third data set was collected by Torardi on $Ca_{14}ZnSb_{11+x}$ obtained from yet another preparation. Room-

(24) Sheldrick, G. M. *XEMP, SHELXTL PLUS*, a program for an empirical absorption correction, Version 4.2, Siemens Analytical X-ray Instruments, Madison, WI, 1990.

Table 5. Selected Bond Lengths (Å) and Angles (deg) for $Sr_{14}ZnSb_{11}$ and $Sr_{14}CdSb_{11.37}$

	$Sr_{14}ZnSb_{11}$	$Sr_{14}CdSb_{11.37}$
Sb(1)–Sb(4)	3.152(8)	3.126(14)
Sb(1)–Sb(4′)	3.523(8)	3.591(14)
Sb(1)–Sr(1) × 2	3.350(2)	3.380(2)
Sb(1)–Sr(2) × 2	3.461(2)	3.461(1)
Sb(1)–Sr(3) × 2	3.522(1)	3.545(1)
Sb(1)–Sr(4) × 2	3.393(2)	3.421(2)
Sb(2)–M(1)	2.806(1)	2.909(1)
Sb(2)–Sr(1)	3.375(2)	3.347(2)
Sb(2)–Sr(1′)	3.391(2)	3.380(2)
Sb(2)–Sr(2)	3.265(2)	3.296(2)
Sb(2)–Sr(2′)	3.873(2)	4.016(3)
Sb(2)–Sr(3)	3.479(2)	3.437(2)
Sb(4)–Sr(4)	3.307(2)	3.330(2)
Sb(4)–Sr(4′)	3.509(2)	3.513(3)
Sb(3)–Sr(1)	3.391(2)	3.365(2)
Sb(3)–Sr(1′)	3.400(2)	3.413(2)
Sb(3)–Sr(2)	3.339(2)	3.349(2)
Sb(3)–Sr(2′)	3.448(2)	3.433(3)
Sb(3)–Sr(3)	3.309(2)	3.319(2)
Sb(3)–Sr(4)	3.338(2)	3.366(2)
Sb(3)–Sr(4′)	3.999(3)	4.009(3)
Sb(3′)–Sb(3)	0.713(9)	
Sb(3′)–Sb(3)	2.978(22)	
Sb(4)–Sb(4′)	0.372(8)	0.465(14)
Sb(4)–Sr(1) × 2	3.281(4)	3.262(4)
Sb(4)–Sr(1′) × 2	3.467(5)	3.491(5)
Sb(4)–Sr(2) × 2	3.520(4)	3.532(5)
Sb(4)–Sr(2′) × 2	3.705(5)	3.770(5)
Sb(5)–Sb(1)		3.064(14)
Sb(5)–Sb(2)		3.181(14)
Sb(5)–Sb(3)		2.899(14)
Sb(5)–Sb(3)		3.390(14)
Sb(5)–Sr(1)		2.875(14)
Sb(5)–Sr(2)		2.876(14)
Sb(5)–Sr(2′)		2.921(14)
Sb(5)–Sr(4)		2.632(14)
Sb(2)–M–Sb(2′)	104.96(2)	105.00(2)
Sb(2)–M–Sb(2″)	118.96(4)	118.85(5)

temperature data were obtained from a CAD-4 diffractometer (Mo Kα radiation). The refinement of the $A_{14}MSb_{11}$ structure proceeded uneventfully and a residual peak of approximately 10 $e^-/Å^3$ was again present in the Fourier difference map. This time the residual peak was on the 16e site, not the 32g site, with the atomic coordinates x, y, z = 0.1401, 0, 0.25. The structure was refined to R = 5.08%, Rw = 4.43% for 801 reflections with $I > 3\sigma(I)$ in the space group $I4_1/acd$, with Sb(5) on the 16e site. The final stoichiometry for this crystal was also $Ca_{14}ZnSb_{11.20}$. Lattice parameters for this crystal, a = 16.620(3) and c = 22.85(1), were significantly different from those obtained from the two crystals for which single-crystal X-ray data were collected at UCD, although unit-cell volume comparisons showed only a 1% difference. The difference in lattice constants was not observed in Guinier X-ray powder diffraction patterns.

A second data set (one octant (hkl), $2\theta_{max} = 55°$) collected for $Ca_{14}CdSb_{11+x}$ was followed by a different absorption program, XABS,[25] after the convergence of isotropic U's. This data set yielded similar results to those described above. A second data set (one octant (hkl), $2\theta_{max} = 65°$) collected for $Sr_{14}CdSb_{11+x}$ employed $\theta-2\theta$ scans and an analytical absorption[26] correction was applied. Again, the results obtained for $A_{14}CdSb_{11+x}$ showed additional electron density compared to the $Ca_{14}AlSb_{11}$ structure type which could be best modeled as Sb. In conclusion, with the exception of $Ca_{14}ZnSb_{11+x}$, regardless of the amount of data or type of absorption correction, the results of the additional data set are identical to those of the first for each compound.

The stoichiometries obtained from the refined structures are $Ca_{14}ZnSb_{11.20}$, $Ca_{14}CdSb_{11.43}$, $Sr_{14}ZnSb_{11}$, and $Sr_{14}CdSb_{11.37}$, and these formulas will be used hereafter.

Resistivity. Suitable single crystals were isolated in a nitrogen-filled drybox equipped with a microscope. Crystals were placed on a small piece of alumina in which four 0.002 in. diameter platinum leads were attached. The leads were mounted on the crystal with silver epoxy. The epoxy was then cured by transferring the crystal (under N_2) to a furnace and heated to 100 °C for 1 h under vacuum. The crystal was then transferred back to the drybox and Apeazon grease was applied in order to minimize air exposure during transfer from the drybox for resistivity measurements. The sample was mounted on a closed-cycle refrigerator and the sample chamber evacuated. The temperature-dependent d.c. resistivity was measured using the four-probe technique and samples were measured from 15 to 300 K, in 5 K increments. The resistivity apparatus has been described in detail previously,[27] and data were collected with the program DCRES.[28] Minimization of thermal voltages was achieved by reversal of current bias. All samples exhibited ohmic behavior.

Results and Discussion

Synthesis. $A_{14}MSb_{11+x}$ can be prepared from the reaction of the elements in the ratio 14:1:11 (A:M:Sb) at 1000 °C. Microprobe data were obtained on several crystals in order to verify the single-crystal X-ray diffraction results. The Sr compounds were too air sensitive to obtain meaningful microprobe data. The air sensitivity of the Sr samples was evidenced by the lack of smooth surfaces in the backscattered image and the low total weight percent obtained in the analysis. It was found that the Sr compounds would decompose within hours even under Paratone oil. Microprobe data on the Ca compounds gave the following results: $Ca_{14.0(1)}Zn_{1.04(5)}Sb_{11.1(1)}$ and $Ca_{14.0(1)}Cd_{1.19(7)}Sb_{11.3(9)}$. There is no evidence for Nb or O, which might come from the reaction container or adventitiously, in these crystals. Within standard deviation, microprobe data indicated that $Ca_{14}ZnSb_{11+x}$ is stoichiometric with $x = 0$ and that $Ca_{14}CdSb_{11+x}$ has additional Cd. This is not in agreement with the results from single-crystal X-ray diffraction which provides the formulas $Ca_{14}ZnSb_{11.20}$ and $Ca_{14}CdSb_{11.43}$. This group has successfully used microprobe data to confirm single-crystal X-ray refinement[8] results, so lack of confirmation is surprising. The large errors for $Ca_{14}CdSb_{11+x}$ indicate inhomogeneity but may also be due to the crystals not lying flat or to the standards used. The microprobe data suggests that stoichiometries vary somewhat for different crystals.

Since microprobe only ruled out the presence of Nb and O, a number of different reactions were run in order to provide additional verification of the single-crystal X-ray diffraction results. Reactions were investigated with the intended stoichiometry $A_{14}MSb_{11}O_{2-x}$. The small amount of oxygen was introduced by using stoichiometric amounts of ZnO or CdO instead of the pure metals, and these reactions produced new diffraction patterns that could not be identified as the $Ca_{14}AlSb_{11}$ structure type or any known oxide. The product was

(25) Hope, H.; Moezzi, B. *XABS*, program provides an empirical correction based on F_o and F_c differences, Chemistry Department, University of California, Davis, 1987.

(26) Sheldrick, G. M. *SHELXTL-PLUS*, Faced indexed numerical analytical absorption correction, Version 4.0, Siemens Analytical X-ray Instruments, Madison, WI, 1990.

(27) Sunstrom, J. E.; Kauzlarich, S. M.; Klavins, P. *Chem. Mater.* **1992**, *4*, 346.

(28) Sunstrom, J. E. IV, *DCRES*, QuickBASIC program for resistivity data collection and statistical analysis, University of California, Davis, unpublished, 1990.

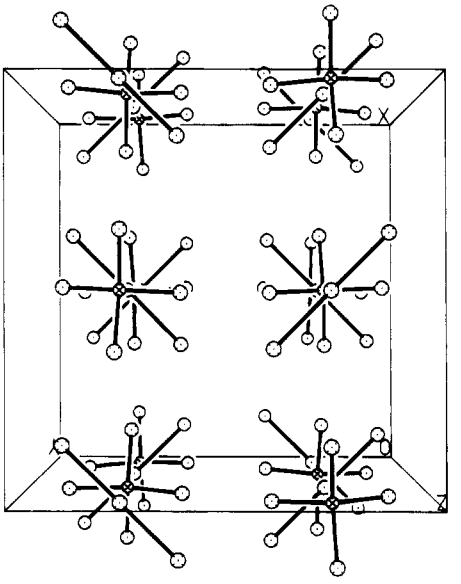

Figure 2. Perspective view down the c axis showing the relative orientation of the $AlSb_4$ tetrahedra and Sb_3 units. The Sb and Al atoms are indicated by dotted and cross-hatched circles, respectively.

inhomogeneous, and no crystals were formed. The addition of Sb_2O_3 yielded a similar result, and these reactions were not pursued further. These results provide convincing evidence that oxygen is not necessary for synthesis of the compounds and therefore is not present in the structure.

Products of reactions with stoichiometric amounts of the elements as determined by single crystal X-ray diffraction could be identified as the $Ca_{14}AlSb_{11}$ structure type. In the case of $Ca_{14}ZnSb_{11+x}$, of the three crystals for which diffraction data were collected, one showed significant differences in the lattice parameters compared to the other two (a = 16.620(3) Å and c = 22.85(1) Å versus a = 16.778(3) Å and c = 22.088(6) Å). However, the lattice parameters obtained from the room-temperature Guinier powder diffraction patterns were the same for all three reactions. Also, there are no significant differences in the intensities of the diffraction peaks for calculated powder patterns of any one compound with or without Sb(5). Lattice parameters obtained from Guinier powder X-ray diffraction were, within 1 standard deviation, the same for reactions prepared from stoichiometric amounts of the elements versus the compositions obtained from single-crystal X-ray diffraction. Different preparation of the $A_{14}MSb_{11+x}$ compounds also yielded the same lattice parameters. The small amount of additional element necessary to obtain high yields of the desired compound is easily satisfied by small errors in the mass of the reagents.

Structure. Figure 2 shows the polyatomic anions of the $Ca_{14}AlSb_{11}$ structure type which consists of columns of alternating MSb_4^{9-} tetrahedra and Sb_3^{7-} linear chains that are coincident to the c axis. As the tetrahedra and linear chains alternate, the linear chains are staggered 90° with respect to each other and the tetrahedra are eclipsed along the c axis. In Figure 3 parts a and b, a perspective view down the c and a axes, respectively, show the isolated Sb^{3-} anions with the coordinated cations which are located between the tetrahedra/linear chain columns. The isolated Sb^{3-}

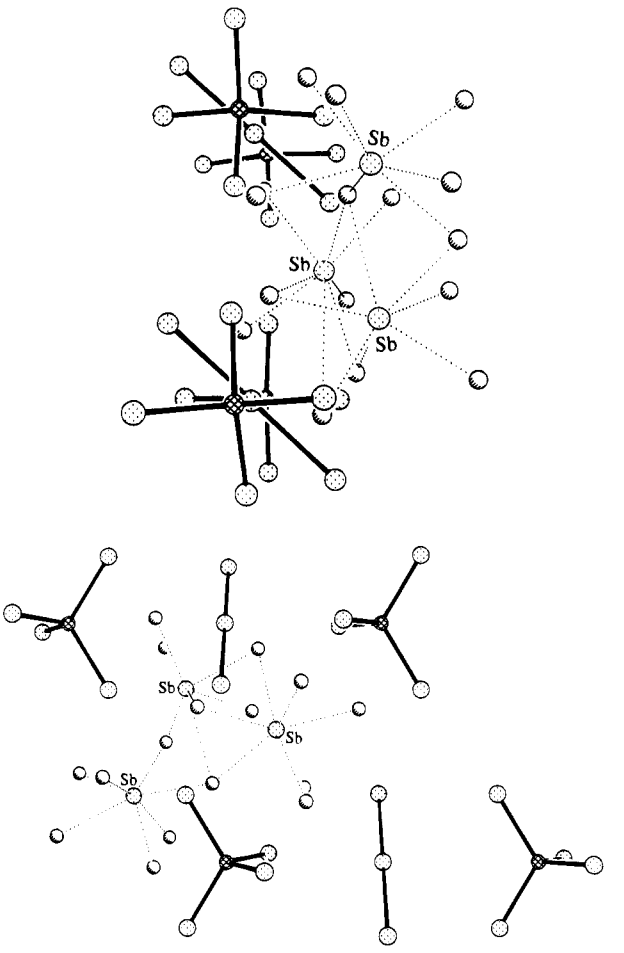

Figure 3. (a, top) Perspective view down the c axis. (b, bottom) a axis, showing the location of the isolated Sb^{3-} anions with the coordinated cations and the tetrahedra/linear chain columns. The Sb, M, and A atoms are indicated by random dotted, cross-hatched, and half-shaded circles, respectively.

anions spiral down the c axis in which the shortest distance to a neighboring Sb^{3-} anion is too long (4.138–4.326 Å in $Ca_{14}AlSb_{11}$)[5] to be considered a bond. The structure has been described in detail elsewhere,[5] and formal charges for one formula unit are counted as 14 Ca^{2+} cations + $[AlSb_4]^{9-}$ + $[Sb_3]^{7-}$ + 4 $[Sb]^{3-}$. Although compounds with the stoichiometry $A_{14}MnPn_{11}$ (A = Ca, Sr, Ba and Pn = As, Sb, Bi) show unusual electronic and magnetic behavior,[11–14,29,30] the main group analogues are all semiconductors and are therefore considered Zintl compounds.[8–10]

In considering the compounds, $A_{14}MSb_{11}$ (A = Ca, Sr and M = Zn, Cd), the highest positive formal oxidation state available for Zn and Cd is 2+. Therefore these compounds would be electron deficient and in the simplest case, one might expect them to be isostructural to the other compounds already reported for this structure and have metallic behavior. Upon investigating the structures of these compounds, we were surprised by the nonstoichiometry and the lack of a consistent structural solution to these isoelectronic compounds. Tables 4 and 5 give bond distances and angles. Ca_{14}-

(29) Kuromoto, T. Y.; Kauzlarich, S. M.; Webb, D. J. *Mol. Cryst. Liq. Cryst.* **1990**, *181*, 349.
(30) Siemens, D. P.; Del Castillo, J.; Potter, W.; Webb, D. J.; Kuromoto, T. Y.; Kauzlarich, S. M. *Solid State Commun.* **1992**, *84*, 1029.

$ZnSb_{11.20}$, $Ca_{14}CdSb_{11.43}$, $Sr_{14}ZnSb_{11}$, and $Sr_{14}CdSb_{11.37}$ are similar to $A_{14}MPn_{11}$ analogs in that tetrahedra ($[ZnSb_4]^{10-}$, $[CdSb_4]^{10-}$) and linear chain $[Sb_3]^{7-}$ anionic subunits are present. Differences lie in deviations from ideal stoichiometry and charge-counting schemes. These differences are attributed to the electron deficiency caused by the inability of Zn and Cd to fill the electronic requirement of the structure type. Figure 4 shows the volumes of all the $A_{14}MSb_{11}$ compounds crystallizing in the $Ca_{14}AlSb_{11}$ structure. The largest deviation in volume for the $Ca_{14}CdSb_{11.43}$ compound which has the largest amount of additional Sb. The small volume observed for $Sr_{14}ZnSb_{11}$ may be attributed to bonding interactions and will be discussed further below.

Figure 3 shows the stacking and coordination of the anionic units. Focusing on general trends, tetrahedral M−Sb bond lengths increase as the metal size increases. Zn−Sb bond distances (2.752(1) Å (Ca) and 2.806(1) Å (Sr)) are shorter than Cd−Sb bond distances (2.882(1) Å (Ca) and 2.909(1) Å (Sr)) as expected due to the smaller covalent radius of the metal. These distances are comparable to ternary compounds containing Zn−Sb and Cd−Sb bonds.[31] The M−Sb distances within each metal series also lengthen as a function of increase alkaline earth cation size and electron donating ability. Likewise, lengthening of the M−Sb bond is observed when the $A_{14}AlSb_{11}$[8] and $A_{14}MnSb_{11}$[13] analogs are compared to each other. The tetrahedral angles in the MSb_4 unit are far from ideal, yet the Zn and Cd compounds show approximately the same amount of tetrahedral distortion regardless of the alkaline earth cation or metal size: $Ca_{14}ZnSb_{11.20}$, 105.26(2)° and 118.96(4)°; $Sr_{14}ZnSb_{11}$, 104.94(2)° and 118.96(4)°; $Sr_{14}CdSb_{11.37}$, 105.00(2)° and 118.85(5)°. $Ca_{14}CdSb_{11.43}$ is the exception with angles of 107.63(3)° and 110.40(1)°. Similarly, $A_{14}AlSb_{11}$ and $A_{14}MnSb_{11}$ analogs show very little dependence of the tetrahedral angles on cation size.[8,13] These Zn and Cd compounds show the largest deviation from the ideal tetrahedral angle of 109.5° compared to all compounds[8−13] of the $Ca_{14}AlSb_{11}$ structure type. This is curious, since no electronic effects should be important and may be attributed to the presence of Sb(5) in $Ca_{14}ZnSb_{11.20}$ and $A_{14}CdSb_{11+x}$ (A = Ca, Sr) and to the disorder of Sb(3) in $Sr_{14}ZnSb_{11}$. These anions are in close proximity to the tetrahedron and, at the least, effect the alkaline earth cation coordination. Thus far, there are no other examples of isolated $ZnSb_4$ or $CdSb_4$ tetrahedral units in the solid state or otherwise. However, corner-shared anionic $ZnSb_4$ and $CdSb_4$ tetrahedral units are found in Zintl compounds AB_2Sb_2[31] (A = Ca, Sr; B = Zn, Cd). In the AB_2Sb_2 compounds, the angles of tetrahedral units exhibit a minimal amount of distortion, a few examples are $CaZn_2Sb_2$, 108.08(5)° and 110.82(5)°; $CaCd_2Sb_2$, 110.44(4)° and 108.49(4)°.

The Sb_3^{7-} linear chain can be rationalized in terms of either simple VSEPR rules[32] (dsp^3 hybridization) or a hypervalent model[33−35] (three-center four-electron bond). Both arguments account for the Sb−Sb bond elongation observed in the Sb_3 linear chain unit. In the VSEPR model, elongation is achieved by electron−electron repulsions between lone pairs on the central Sb atom and terminal Sb atoms; and in the hypervalent model, the bond order of the central to terminal Sb is 1/2. All other $A_{14}MPn_{11}$ compounds of the $Ca_{14}AlSb_{11}$ structure type exhibit an increase in the Pn−Pn bond distance of the Pn_3^{7-} linear chain, as the cation size and electron donor ability increases.[8−10,12,13] The single crystal X-ray data for both $Sr_{14}ZnSb_{11}$ and $Sr_{14}CdSb_{11.37}$ is best fit with a disordered model which makes the Sb_3^{7-} unit asymmetrical with two inequivalent distances for Sb(1)−Sb(4). This has also been observed in $Sr_{14}GaAs_{11}$[10] and $Ba_{14}MnSb_{11}$.[13] Apparently the Sb−Sb distance in the Sb_3 unit is too long for a symmetrical bonding arrangement. If one idealizes the position of Sb(4) in the Sr analogs and compares the symmetrical bond lengths, then the average Sb−Sb bond lengths in the Sb_3^{7-} linear chains increase with increasing cation size and donor ability. In the Zn compounds the average Sb−Sb bond lengthens by about 0.1 Å, 3.231(1) Å (Ca) and 3.335(8) Å (Sr, idealized Sb(4) position). The same trend is observed in the Cd analogs, 3.180(1) Å (Ca) and 3.36(2) Å (Sr, idealized Sb(4) position). This increase is attributed to increased size and electron donation ability of the cation. Comparing the Ca analogs, the Sb−Sb bond distance is slightly shorter for the Cd versus Zn compound. In the case of the Sr analogs, the opposite effect is observed: the Sb−Sb distance is slightly shorter for the Zn versus the Cd compound. This may be due to the differences in the nonstoichiometry for each compound.

The environment of the Sb^{3-} isolated anion is similar for Zn and Cd compounds. Figures 3a and 3b show the relative orientation of Sb^{3-} with respect to the tetrahedra and linear units in the $Ca_{14}AlSb_{11}$ structure. Sb^{3-} has a coordination sphere of seven cations as shown in Figure 3. The only compound that shows disorder of this atom is $Sr_{14}ZnSb_{11}$ and will be discussed in detail below. The shortest Sb to cation distances in the Zn analogs are 3.163(3) Å (Ca) and 3.309(2) Å (Sr). In the Cd compounds, the shortest distances are 3.137(2) Å (Ca) and 3.319(2) Å (Sr). Typical Sb−Ca and Sb−Sr distances in other ternary Zintl compounds $Ca_9Zn_4Sb_9$[36] and $SrZn_2Sb_2$[31] range from 3.172(4) to 3.699(5) Å and 3.324(1) to 3.353(1) Å, respectively. These distances are consistent with viewing the alkaline-earth cation as a two-electron donor.

$Sr_{14}ZnSb_{11}$ exhibits a positional disorder in the Sb^{3-} anion that is not observed in any of the other analogs. The Sb^{3-} anion is best modeled as Sb(3) 85% and Sb(3′) 15% in which Sb(3′) is approximately 0.7 Å away from Sb(3). Sb(3′) is 2.978(22) Å away from another Sb(3) atom and thus forms Sb−Sb dimers that spiral down the *c* axis. This 2.978 Å Sb−Sb distance is considered bonding, since this distance is shorter than the observed bond lengths in the Sb_3 unit (3.126(14)−3.231(1) Å, for Zn and Cd compounds discussed previously) and comparable to elemental Sb (Sb−Sb = 2.90 Å). Formally, one would consider this a Sb_2^{4-} anion. The structure could then be considered composed of about 85% isolated Sb^{3-} anions (four in a formula unit) and 15% Sb_2^{4-} anions (two in a formula unit). This increase in bonding

(31) Mewis, A. *Z. Naturforsch.* **1978**, *33b*, 1978.
(32) Huheey, J. E. *Inorganic Chemistry: Principles of Structure and Reactivity*; Harper and Row: New York, 1983; p 118.
(33) Musher, J. I. *Angew. Chem., Int. Ed. Engl.* **1969**, *8*, 54.
(34) Pimental, G. C. *J. Chem. Phys.* **1951**, *19*, 446.
(35) Rundle, R. E. *Surv. Prog. Chem* **1963**, *1*, 81.
(36) Brechtel, E.; Cordier, G.; Schäfer, H. *Z. Naturforsch.* **1981**, *36b*, 1099.

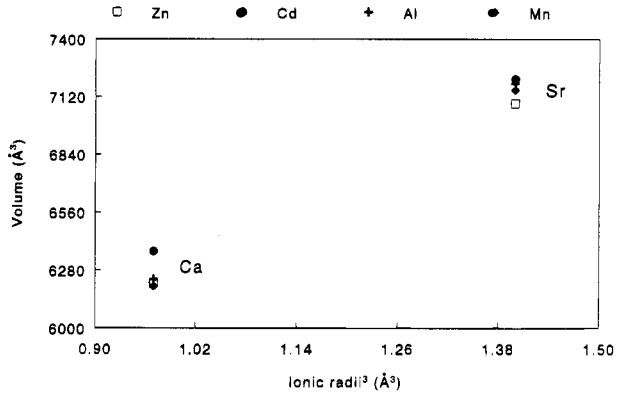

Figure 4. Plot of cell volume versus ionic radii cubed for $A_{14}MSb_{11}$ and $A_{14}MSb_{11+x}$.

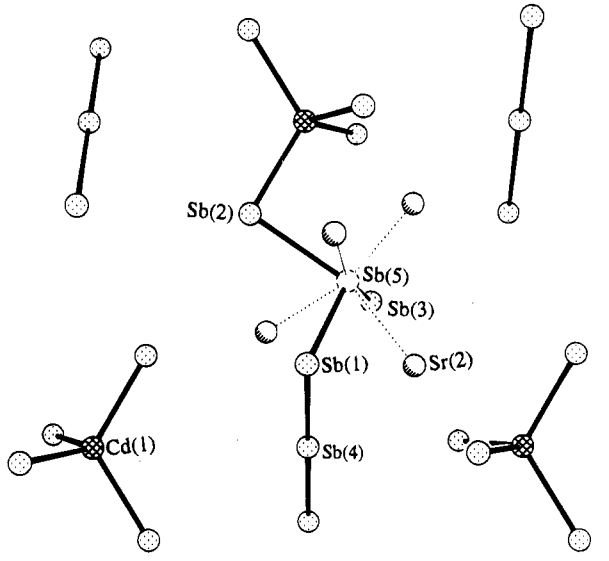

Figure 5. View down the *a* axis showing the location of Sb(5) in $Sr_{14}CdSb_{11.37}$ and $Ca_{14}ZnSb_{11.20}$.

may account for the contraction in volume observed in Figure 4.

The environment of the additional Sb, Sb(5), in all these compounds is similar. There are two different crystallographic sites for the additional Sb, 32g and 16e. There are four nearest-neighbor Sb's giving Sb(5) an approximately tetrahedral coordination, and the average bond lengths are similar. $Ca_{14}ZnSb_{11+x}$ apparently

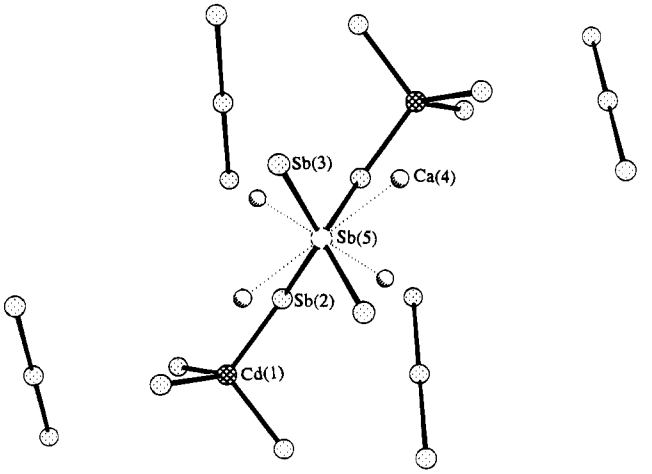

Figure 6. View down the *a* axis showing the location of Sb(5) in $Ca_{14}CdSb_{11.43}$.

can crystallize with the additional Sb in either of these sites. This implies that the sites are similar in energy. In the case of the Sb in the 32g site in $Ca_{14}ZnSb_{11+x}$ and $Sr_{14}CdSb_{11.37}$, Sb(5) is positioned within bonding distances to only three other Sb atoms to form a trigonal pyramid, see Figure 5. The Sb(5) is bonded to one terminal Sb(1) atom of a linear chain, one corner Sb(2) atom of a tetrahedron, and an isolated Sb(3) atom. The addition of Sb(5) in these compounds may account for the longer Sb–Sb distance observed in the Sb_3^{7-} unit for Zn vs Cd (Ca analog) and Cd vs Zn (Sr analog). In $Ca_{14}ZnSb_{11.20}$, Sb(5)–Sb distances are 2.920(22), 2.948(22), and 2.746(21) Å; in $Sr_{14}CdSb_{11}$, Sb(5)–Sb distances are 3.064(14), 3.181(14), and 2.899(14) Å. Sb(5)–Sb(3), 2.746(21) Å, in $Ca_{14}ZnSb_{11.20}$ is shorter than the Sb–Sb distances discussed thus far; however, it is not considered unusual since short Sb–Sb bond lengths (2.688(1) Å) have been reported in other Zintl Sb ions.[37] In addition, trigonal Sb–Sb coordination in Zintl Sb ions[38–40] has been reported in which the shortest Sb–Sb distance is 2.70 Å.[38]

$Ca_{14}CdSb_{11.43}$ and one crystal of $Ca_{14}ZnSb_{11+x}$ contains additional Sb, Sb(5), in site 16e. Although, its coordination is similar to Sb(5) in $Ca_{14}ZnSb_{11.20}$ and $Sr_{14}CdSb_{11.37}$, there are four Sb atoms within bonding distance, see Figure 6. Sb(5) is tetrahedrally coordinated to four Sb atoms, two Sb(2) atoms from different tetrahedra, and two Sb(3) isolated atoms. The bond distances range from 2.693(2) to 3.258(3) Å.

Resistivity. Resistivity measurements were obtained for single-crystal samples for all compounds and all show typical semiconductor behavior. $A_{14}MSb_{11+x}$ forms silver opaque crystals that have a high luster, indicating that these compounds might be narrow-gap semiconductors. Figure 7 shows ln ϱ vs $1/T$ data for the Zn and Cd compounds made. The room-temperature resistivities are $Ca_{14}ZnSb_{11.20}$, $3.5(1) \times 10^{-1}$ Ω cm; $Sr_{14}ZnSb_{11}$, 6.0(1) Ω cm; $Ca_{14}CdSb_{11.37}$, $2.8(1) \times 10^{-1}$ Ω cm; $Sr_{14}CdSb_{11.43}$, $6.3(1) \times 10^{-1}$ Ω cm. Data were collected over the temperature range 300–15 K, and at low temperature, saturation effects were observed. Activation energies obtained from fitting the data from 55 to 300 K to the equation, $\ln \varrho = E_a/2k_BT + \varrho_0$ and, along with room-temperature resistivities, are given in Table 6. The relatively small room-temperature resistivities and activation energies are the same order of magnitude as observed for the $A_{14}Al_{1-x}Sb_{11+x}$ compounds.[8] As mentioned previously, the Sr and Ba aluminum compounds show substituted disorder with about 5–10% Sb^{3+} replacing Al^{3+} in the structure. The low ϱ and small E_a observed for the $A_{14}AlSb_{11+x}$ compounds are attributed to this substitutional disorder. The small room-temperature resistivities and activation energies observed for the $A_{14}MSb_{11+x}$ compounds are probably due to the nonstoichiometry of the samples and suggest that these compounds are either heavily doped semiconductors or semimetals. Absorption bands were observed in the expected region of the far-IR.

(37) Evans, W. J.; Gonzales, S. L.; Ziller, J. W. *J. Chem. Soc., Chem. Commun.* **1992**, 1138.
(38) Adolphson, D. G.; Corbett, J. D.; Merryman, D. J. *J. Am. Chem. Soc.* **1976**, *98*, 7234.
(39) Critchlow, S. C.; Corbett, J. D. *Inorg. Chem.* **1984**, *23*, 770.
(40) Bolle, U.; Tremel, W. *J. Chem. Soc., Chem. Commun.* **1992**, 91.

Table 6. Activation Energies and Room-Temperature Resistivities

compound	crystal size (mm)	E_a (eV)	ϱ_{300K} (Ω cm)	ϱ_0
$Ca_{14}ZnSb_{11.20}$	1.3 × 0.07 × 0.07	3.6(1) × 10^{-4} (160–300 K)	3.4(1) × 10^{-2}	−3.42(1)
$Ca_{14}CdSb_{11.43}$	2.4 × 0.04 × 0.04	7.6(1) × 10^{-2} (175–300 K)	2.8(1) × 10^{-2}	−2.73(1)
$Sr_{14}ZnSb_{11}$	1.1 × 0.3 × 0.3	2.7(1) × 10^{-2} (165–300 K)	6.0(1)	1.14(1)
$Sr_{14}CdSb_{11.37}$	1.5 × 0.05 × 0.05	1.6(1) × 10^{-2} (160–275 K)	6.3(1) × 10^{-1}	−0.69(1)

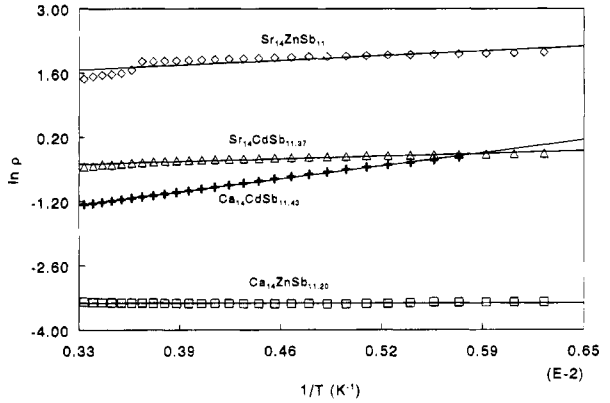

Figure 7. ln ϱ versus $1/T$ (T = 153–300 K) of single crystals $A_{14}MSb_{11+x}$.

Electron Counting. Zintl compounds are rationalized as ionic salt-like compounds, yet those composed of the heavier elements can show metallic bonding and are considered to be intermetallic. Zintl electron counting assumes that the electropositive elements, alkali metals, or alkaline earths are simple electron donors. Intermetallics on the other hand, show clustering of the electropositive elements and electron counting is not quite so simple. For example in $Mg_6Cu_{16}Si_7$, Mg atoms form polyhedra that are counted as $[Mg_6]^{4+}$ and the Mg–Mg distances are short (2.00 Å). In the $A_{14}MSb_{11+x}$ compounds the cation–cation distances are too long for them to be considered in this manner. In addition, Figure 4 shows that there is no discrepancy in volume with the exception of $Sr_{14}ZnSb_{11}$ that might indicate a distinctly different type of bonding in these compounds compared with others of the $Ca_{14}AlSb_{11}$ structure.

Can we account for the structure and bonding in these Zn and Cd $A_{14}MSb_{11+x}$ compounds using Zintl rules? In the simplest case of valence precise $A_{14}AlSb_{11}$, Al is formally in a +3 oxidation state, and connectivities are easily rationalized by Zintl rules. As mentioned previously, one formula unit is described as consisting of 14-$[Ca^{2+}]$ + $[AlSb_4]^{9-}$ + $[Sb_3]^{7-}$ + 4$[Sb^{3-}]$. Theoretical calculations on $Ca_{14}GaAs_{11}$[41] have shown that the Zintl concept accurately describes the bonding in this structure type. However, if we adhered to an analogous Zintl counting scheme in the Zn and Cd analogs, ignoring the disorder Sb(3) in $Sr_{14}ZnSb_{11}$ and the extra Sb, Sb(5), in the other compounds, charges would be counted as follows: 14$[A^{2+}]$ + $[MSb_4]^{10-}$ + $[Sb_3]^{7-}$ + 4$[Sb^{3-}]$, the cationic charge is deficient by +1. The Zn and Cd series exhibit the correct properties to be considered Zintl compounds (semiconducting), and this suggests that, neglecting d electrons, one should be able to rationalize connectivities and describe these compounds as valence compounds.

The simplest compound to electron count in this series is $Sr_{14}ZnSb_{11}$. In $Sr_{14}ZnSb_{11}$, recall that Sb(3), isolated Sb^{3-}, is positionally disordered and that the situation can be modeled 85% 4$[Sb]^{3-}$ and 15% 2$[Sb\text{-}Sb]^{4-}$. Since Sb(3) and Sb(3′) are highly correlated, a reasonable model with similar R, wR2 is also obtained restricting the occupancy to 75% 4$[Sb]^{3-}$ and 25% 2$[Sb–Sb]^{4-}$ (75% Sb(3), 25% Sb(3′)). In this idealized case, the charge counting would follow the scheme 14$[Sr^{2+}]$ + $[ZnSb_4]^{10-}$ + $[Sb_3]^{7-}$ + 0.75{4$[Sb]^{3-}$} + 0.25{2$[Sb–Sb]^{4-}$} = (+28) + (−10) + (−7) + (−9) + (−2). This model suggests that the positional disorder of Sb(3) is necessary in order to balance charge.

In $Ca_{14}ZnSb_{11.20}$, $Ca_{14}CdSb_{11.43}$, and $Sr_{14}CdSb_{11.37}$ a different mechanism must be invoked to balance electrons. It is surprising that all the compounds do not simply employ the same scheme as suggested above to satisfy the electron counting. In fact, the $Sr_{14}ZnSb_{11}$ compound was synthesized first, and the $Sr_{14}CdSb_{11}$ compound subsequently in order to provide further verification of the disorder for Sb(3). Since a new problem of nonstoichiometry arose, the Ca analogs were then synthesized also. In all of these compounds, there is the problem of the extra Sb, Sb(5). The nonstoichiometry is probably due to the electron deficiency. In the simplest construction, if we consider Sb(5) to be a Sb^{3+} cation we would need 0.33 of an Sb to obtain the missing +1 charge. Although $Ca_{14}ZnSb_{11.20}$ is slightly deficient with 0.2 of an additional Sb (Sb^{3+}), both $Ca_{14}CdSb_{11.43}$ and $Sr_{14}CdSb_{11.37}$ are approximately of the correct stoichiometry to balance formal charges.

In summary, although this structure type can be described according to Zintl electron-counting rules, it can adapt in order to accommodate a +2 metal. Three variations of the structure were presented, as determined by single-crystal X-ray diffraction. $Ca_{14}ZnSb_{11+x}$ can crystallize in the $Ca_{14}AlSb_{11}$ structure type with an additional atom located in either the 32g or the 16e site, suggesting that the energy difference between the two sites is minimal. A structural model with Sb as the additional atoms provides the most rational coordination sphere and distances to neighboring atoms. All compounds exhibit semiconducting behavior. The simplest interpretations of these structures with regards to electron counting were discussed. A theoretical study is warranted on these compounds and will provide new insight into the bonding of these unusual compounds.

Acknowledgment. This research was funded by the National Science Foundation, DMR-9201041. We thank Professor Håkon Hope for useful discussion and Professor Anne Hofmeister for the far IR data.

(41) Gallup, R. F.; Fong, C. Y.; Kauzlarich, S. M. *Inorg. Chem.* **1992**, *31*, 115.